

THE ABSORPTION OF H₂ AND CO FROM BUBBLES IN A GLASS MELT

LUBOMÍR NĚMEC, JAROSLAV KLOUŽEK

Laboratory of Inorganic Materials of the Institute of Inorganic Chemistry ASCR and the Institute of Chemical Technology,
Technická 5, 166 28 Prague

E-mail: Lubomir.Nemec@vscht.cz

Submitted July 7, 2000; accepted September 20, 2000.

Hydrogen and carbon monoxide bubbles in a glass melt are produced by reactions of carbon, iron and ferrous oxide impurities with oxygen or water vapour. Their modelling in melting space joined with defect bubble analyses could help to identify the appropriate bubble defect source, however, mechanisms of bubble interactions with melts are not yet known. The experimental examination of bubbles initially containing 95 vol.% H₂ and 5 vol.% N₂ showed a rapid absorption of hydrogen by the melt. The proposed mechanism of interaction involved the controlling role of hydrogen and oxidizing components counter-diffusion in bubble surroundings and influence of chemical reaction of hydrogen with the mentioned oxidizing melt components (O₂, sulphate ions). The governing equations of this phenomenon were presented, as well as a simplified mechanism applying the value of hydrogen effective diffusion coefficient under given value of the redox state of glass. Using the results of experimental observations, the temperature dependencies of the product of effective diffusion coefficient and solubility of hydrogen - necessary for the modelling of bubbles containing hydrogen - were determined in soda-lime-silica glass containing 0.5 wt.% SO₃ ($D_{H_2,eff}^{2/3} L_{H_2} = \exp(0.866-7438/T)$) and amber glass ($D_{H_2,eff}^{2/3} L_{H_2} = \exp(0.946-9125/T)$), where T is temperature in Kelvins.

INTRODUCTION

The examination of interactions between multi-component bubbles and glass melts provides a very comprehensible picture of interaction between gases and glass melts generally. The main reason of this fact is the relatively easy measurement of bubble volume changes by direct observations [1], the chance to analyse gas content of bubbles, as well as a good theoretical background [2 - 5]. In addition, bubbles play an ill fated role of the most significant defect of industrial glasses. As the defect history during the melting process deeply affects bubble frequency in products, the bubble examination at melting temperatures has also a practical important consequence.

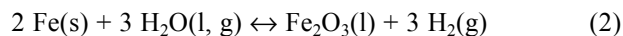
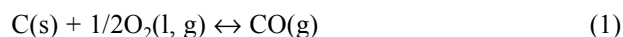
A considerable effort has been paid to the behaviour of bubbles containing gases typical for characterisation of the industrial melting process, as was CO₂, N₂, O₂, H₂O, SO₂ and Ar. On the contrary, the knowledge of the behaviour of reactive reducing gases, namely H₂ and CO, was restricted to occasional analytical determination in defect bubbles [6]. Their interactions give nevertheless an interesting example of chemical interaction between a reactive gas and glass melt, impact on the industrial bubble removing process and are significant for the identification of some defect bubble sources during the melting process.

This work is aimed at the examination of the mechanism by which H₂ and CO in bubbles react with a glass melt containing oxidizing components, as is oxygen, and sulphate ions. The experimental examination of contraction of bubbles containing the

mixture of hydrogen and nitrogen in the melt, as well as the GC analyse of gases remaining after absorption of a defined volume of gases in the melt were applied to elucidate the absorption mechanism. The results of experimental observations were used to propose the general governing equations of the reactive bubble interaction with a glass melt, as well as to present the simplified mechanism of contraction of multi-component bubbles containing H₂ and CO.

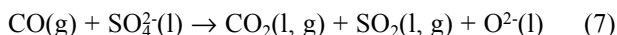
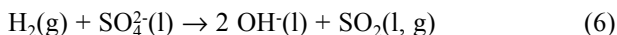
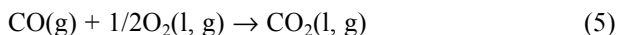
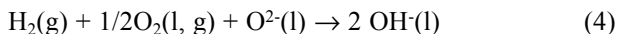
THEORETICAL PART

The reactive gases present in some defect bubbles come from reactions between reducing components present as impurities, namely carbon, iron or ferrous oxide with oxidizing components or water vapour [1]:



If the sulphate ions are present in glass, the subsequent reactions with SO₂ in both bubbles and melt provides COS and H₂S. Both components are frequently found by defect bubble analyses [6], however, the temperature range of this reaction has not been determined yet. Owing to both experimental and theoretical complexity of this interaction, the discussion will be restricted to reactions of hydrogen and carbon monoxide.

If one or both mentioned gases reside in a bubble, no oxidizing component -oxygen or sulphur dioxide – can be present there. Nevertheless, gases can react with the appropriate components dissolved in the bubble surrounding melt according to reactions:



Note that water coming from reactions (4) and (6) reacts to form OH groups in the melt. The reactions with sulphate may proceed up to H₂S and COS production in the surrounding melt.

When examining the absorption of H₂ and CO by the bubble surrounding melt, two mechanisms are suggested:

- The reacting gas (H₂ or CO) diffuses into the melt and reacts there with any oxidizing component. Its concentration in the bubble decreases with time and no or almost no products of this reaction (H₂O or CO₂ etc.) occur in the bubble. The process of absorption is controlled by the transport of H₂, CO and oxidizing components and is influenced by their chemical reactions in the melt.
- The oxidizing components are present in a sufficient amount in the bubble surface layer or their transport from the melt to the bubble surface is fast. The chemical reaction will take place on the bubble boundary and its products will substitute H₂ and CO in the bubble. The process will be controlled by the surface reaction.

The mentioned cases *a*) and *b*) should considerably differ as regards the resulting volume and composition of bubbles. The experiments involving the absorption of bubbles - containing defined content of H₂ or CO - in the melt and bubble analyses may therefore reveal the dominating reaction mechanism.

EXPERIMENTAL PART

Only experiments with H₂ gas were performed owing to the CO high toxicity. The mixture of 95 vol.% H₂ and 5 vol.% N₂ was cautiously blown in the melt by the silica glass capillary to form small bubbles. The bubbles were video-recorded during their rising up to the melt level and their changes of size were subsequently evaluated by the image analyser. The following glass melts were applied in those experiments:

- The soda-lime-silica glass without refining agent.
- The soda-lime-silica containing 0.5 wt.% SO₃ (dissolved as sulphate ions).
- The amber glass.

The temperature of experiments was 1200, 1300 and 1400 °C.

To determine the composition of remaining gases, the experimental arrangement formerly applied for the measurement of diffusion coefficients of gases in glass melts [8] has been used. The sketch of the experimental arrangement is presented in the figure 1. Before the start of absorption, the gas mixture filled the silica glass vessel above the glass level. Subsequently the vessel with the mixture was immersed into the melt. After gas absorption, the vessel with the sealing layer of the melt has been quickly pulled out of the melt and put into a silica glass chamber in the circuit of gas chromatograph. After spontaneous destruction of the vessel, the remaining gases were analysed.

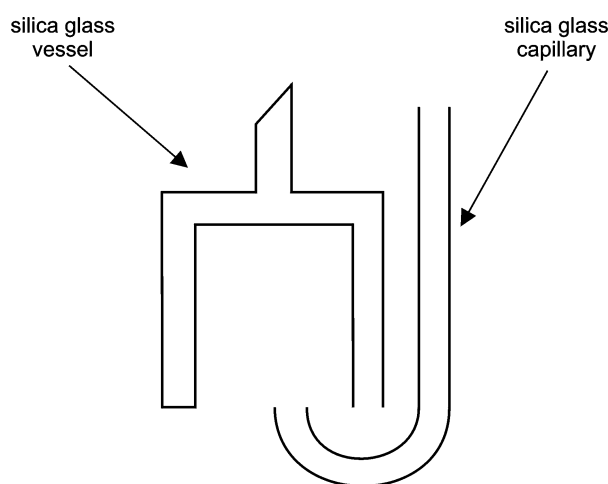


Figure 1. The scheme of experimental arrangement for gas mixture absorption in the melt.

RESULTS

The examples of bubble diameter development with time at different temperatures are presented in figures 2 - 4. The rapid absorption of the bubble content was observed in all cases as well as the increase of the bubble dissolution rate with temperature. The results confirmed the idea of hydrogen absorption controlled by its transport through the surrounding glass (mechanism *a*) in Theoretical part).

The rapid bubble absorption stops after tens of seconds indicating that all or the majority of hydrogen has already penetrated out of the bubble. This fact is confirmed by the table 1, where the absorbed portion of the bubble is presented using the initial and minimum bubble diameter from figures 2 - 4. The absorbed portion of bubble volume corresponded to the initial content of hydrogen or was a little lower. The lower absorbed volume found in several cases was a consequence of partial bubble absorption before bubble left the blowing capillary. This initial bubble absorption was not measured. The values in the table 1 confirm the

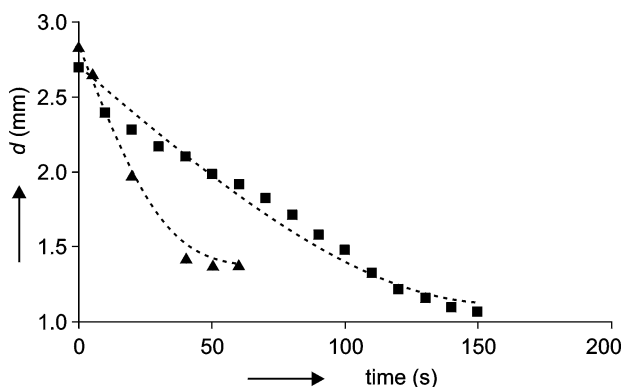


Figure 2. The time development of bubble diameter in the sheet glass melt without refining agent. Initial bubble composition 95 vol.% H₂, 5 vol.% N₂.

■ - 1200 °C, ▲ - 1300 °C, ... calculated courses

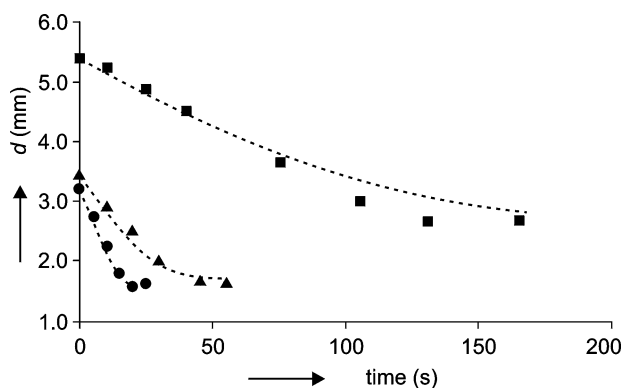


Figure 3. The time development of bubble diameter in the soda-lime-silica glass melt containing 0.5 wt.% SO₃. Initial bubble composition 95 vol.% H₂, 5 vol.% N₂.

■ - 1200 °C, ▲ - 1300 °C, ● - 1400 °C, ... calculated courses

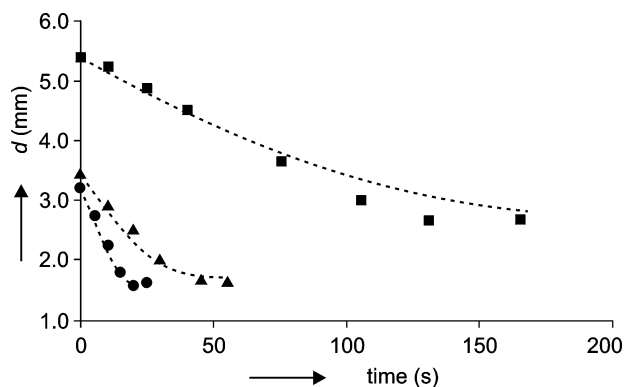


Figure 4. The time development of bubble diameter in the amber glass melt. Initial bubble composition 95 vol.% H₂, 5 vol.% N₂.

■ - 1200 °C, ▲ - 1300 °C, ● - 1400 °C, ... calculated courses

proposed interaction mechanism a) too. The last evidence of the hydrogen transport from bubbles provided analyse of the gas mixture after absorption.

The average composition of the remained gas amounted to 99 vol.% N₂ and 1 vol.% CO₂ (CO₂ occurred from the melt).

Table 1. The absorbed portion of bubbles (%), initially containing 95 vol.% H₂ and 5 vol.% N₂ in the examined glass melts.

	1200 °C	1300 °C	1400 °C
glass without refining agents	93.7	88.7	not measured
glass containing 0.5 wt % SO ₃	87.9	88.5	88.2
amber glass	70.8	67.5	91.7

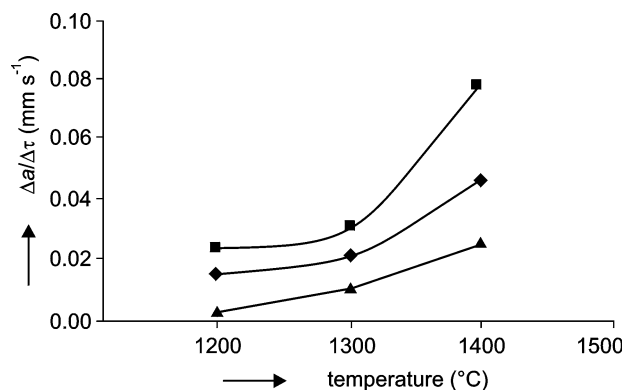


Figure 5. The bubble absorption rate in the examined glass melts versus temperature. Initial bubble compositions are the same as in figures 2 - 4.

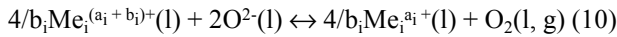
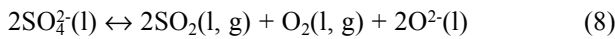
◆ - glass without refining agents, ■ - glass containing 0.5 wt.% SO₃, ▲ - amber glass

The role of chemical reaction in the hydrogen absorption process can be elucidated by comparing the hydrogen absorption rates of three examined glasses having a different redox state. The appropriate temperature dependence of these values is plotted in the figure 5. As is obvious from this figure, the rate of hydrogen absorption increases with increasing redox state of glass, i.e. in the order amber glass, glass without refining agent, glass containing sodium sulphate. These results indicate the importance of chemical reactions (4) and (6) during hydrogen absorption.

DISCUSSION

The experiments with bubble absorption revealed the controlling role of hydrogen diffusion and oxidizing components counter diffusion in the bubble surrounding melt and confirmed the significant effect of the redox state of glass on the rate of absorption.

When searching for the governing equations, the appropriate chemical reactions must be taken into account, namely reactions (4) and (6), if only hydrogen without any carbon monoxide is present in bubbles. Both reactions can be considered fast and irreversible, consequently no oxygen or sulphate ions can be present in the immediate environment of the bubble and, on the contrary, no hydrogen can attain the longer distance from the bubble surface. The schematic picture of hydrogen and oxygen concentration distribution on the radial distance from the bubble (reaction (4)) is presented in the figure 6. Thus, at the distance r' the concentration of both reducing and oxidizing component has almost zero value. In addition to reactions (4) and (6) taking place for $a < r < r'$ (a is the bubble radius), the following reactions are valid when $r > r'$:



where the last oxidation-reduction reaction is mostly represented by the equilibrium between ferrous and ferric ions.

The following set of equations may be proposed for the concentration distributions around a bubble containing hydrogen with nitrogen and rising through the oxidised glass (no sulphide is present):

For hydrogen, sulphur dioxide and nitrogen:

$$\frac{D_i}{r^2} \frac{\partial}{\partial r} \left(r^2 \frac{\partial c_i}{\partial r} \right) - v(r, \Theta) \frac{\partial c_i}{\partial r} = 0; \quad (11)$$

H_2 and SO_2 : $a < r < r'$

N_2 : $r > a$

For sulphur dioxide, oxygen, sulphate ions, ferrous and ferric ions:

$$\frac{D_j}{r^2} \frac{\partial}{\partial r} \left(r^2 \frac{\partial c_j}{\partial r} \right) - v(r, \Theta) \frac{\partial c_j}{\partial r} + \left(\frac{\partial c_j}{\partial \tau} \right)_{\text{ch}} = 0 \quad (12)$$

$\text{SO}_2, \text{O}_2, \text{SO}_4^{2-}, \text{Fe}^{2+}, \text{Fe}^{3+}$: $r > r'$

where $\left(\frac{\partial c_j}{\partial r} \right)_{\text{ch}}$ signifies the change of the j -th concentration component brought about by the shift of equilibria of reactions (8) and (10) owing to the transport of $\text{SO}_4^{2-}, \text{SO}_2, \text{O}_2, \text{Fe}^{2+}$ and Fe^{3+} in the melt, c_i and c_j are the molar concentrations of components in the melt and v is the vector of glass velocity around a rising

bubble. The following relations are valid between $(\partial c_j / \partial \tau)_{\text{ch}}$ resulting from reaction stoichiometry:

$$\begin{aligned} \left(\frac{\partial c_{\text{O}_2}}{\partial \tau} \right)_{\text{ch}} &= -\frac{1}{2} \left(\frac{\partial c_{\text{SO}_4^{2-}}}{\partial \tau} \right)_{\text{ch}} + \frac{1}{4} \left(\frac{\partial c_{\text{Fe}^{3+}}}{\partial \tau} \right)_{\text{ch}} \\ \left(\frac{\partial c_{\text{SO}_2}}{\partial \tau} \right)_{\text{ch}} &= - \left(\frac{\partial c_{\text{SO}_4^{2-}}}{\partial \tau} \right)_{\text{ch}} \\ \left(\frac{\partial c_{\text{Fe}^{2+}}}{\partial \tau} \right)_{\text{ch}} &= - \left(\frac{\partial c_{\text{Fe}^{3+}}}{\partial \tau} \right)_{\text{ch}} \end{aligned} \quad (13)$$

And further in a simplified form:

$$K_{\text{SO}_4^{2-}} = \frac{c_{\text{O}_2} c_{\text{SO}_2}^2}{c_{\text{SO}_4^{2-}}^2}; K_{\text{Fe}} = \frac{(c_{\text{Fe}^{2+}})^4 c_{\text{O}_2}}{(c_{\text{Fe}^{3+}})^4} \quad (14)$$

The appropriate boundary conditions are:

$$\begin{aligned} \tau \geq 0; r < a, p_{\text{H}_2} + p_{\text{N}_2} + p_{\text{SO}_2} &= p_{\text{tot}} \\ r = a, c_{\text{H}_2} = p_{\text{H}_2} L_{\text{H}_2}, c_{\text{N}_2} = p_{\text{N}_2} L_{\text{N}_2}, c_{\text{SO}_2} &= p_{\text{SO}_2} L_{\text{SO}_2}, \\ c_{\text{SO}_4^{2-}} = 0, c_{\text{Fe}^{2+}} = c_{\text{Fe}^{\text{tot}}}, c_{\text{Fe}^{3+}} &= 0 \\ \tau = 0; r = a, c_{\text{SO}_2} = 0; & \\ \tau = 0; r > a, c_{\text{H}_2} = 0; c_{\text{N}_2} = c_{\text{bN}_2}; c_{\text{SO}_4^{2-}} &= c_{\text{bSO}_4^{2-}}, c_{\text{Fe}^{2+}} = \\ = c_{\text{bFe}^{2+}}, c_{\text{Fe}^{3+}} = c_{\text{bFe}^{3+}}, c_{\text{SO}_2} = c_{\text{bSO}_2}, c_{\text{O}_2} &= c_{\text{bO}_2} \\ \tau > 0; r > a, c_{\text{SO}_2} = c_{\text{SO}_2}(\tau), c_{\text{N}_2} = c_{\text{N}_2}(\tau) & \\ a < r < r', c_{\text{H}_2} = c_{\text{H}_2}(\tau), c_{\text{SO}_4^{2-}} = 0, c_{\text{O}_2} = 0; c_{\text{Fe}^{2+}} &= \\ = c_{\text{Fe}^{\text{tot}}}, c_{\text{Fe}^{3+}} = 0 & \\ r > r', c_{\text{H}_2} = 0, c_{\text{SO}_4^{2-}} = c_{\text{SO}_4^{2-}}(\tau), c_{\text{O}_2} = c_{\text{O}_2}(\tau), c_{\text{Fe}^{2+}} &= \\ = c_{\text{Fe}^{2+}}(\tau), c_{\text{Fe}^{3+}} = c_{\text{Fe}^{3+}}(\tau) & \\ r = r', c_{\text{H}_2} = 0, c_{\text{SO}_4^{2-}} = 0, c_{\text{O}_2} = 0 & \end{aligned} \quad (15)$$

and

$$\frac{3}{2} D_{\text{H}_2} \left(\frac{\partial c_{\text{H}_2}}{\partial r} \right)_{r=r'} + D_{\text{O}_2} \left(\frac{\partial c_{\text{O}_2}}{\partial r} \right)_{r=r'} + D_{\text{SO}_4^{2-}} \left(\frac{\partial c_{\text{SO}_4^{2-}}}{\partial r} \right)_{r=r'} = 0 \quad (17)$$

Here p_i and p_{tot} and are the partial pressures of the i -th component and the total gas pressure in the bubble, respectively, L_i is the solubility of the i -th gas component and $c_{\text{Fe}^{\text{tot}}}$ is the total concentration of iron ions in the melt.

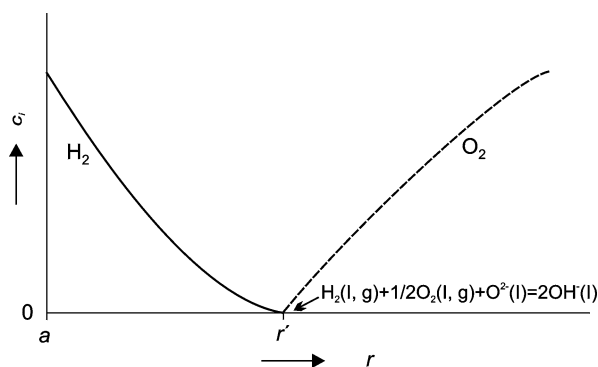


Figure 6. The schematic course of the counter-diffusion of hydrogen from the bubble and oxygen from the glass melt in the bubble surroundings.

The solution does not involve the transport of hydroxyl groups. The concentration of SO₂ in the region $a < r < r'$ could be high, nevertheless no SO₂ was found in bubbles. The role of chemical reactions is probably less significant for amber glass, where the oxygen concentration in the melt is extremely low.

As is clear from the presented theoretical model, the quantitative description of the hydrogen absorption in oxidised glasses is rather complicated both as for the interaction mechanism and numerical solution of proposed equations. When trying to describe the behaviour of multicomponent bubbles containing reducing gases under non-isothermal conditions of flowing glass (bubble defect in glass melting space), an alternative simplified procedure is needed. The proposed procedure assumes the reducing gases behave as non-reacting ones and the expressions for the mass flow between bubbles and melt correspond to those used for non-reacting gases as CO₂, N₂ or Ar. The mass flow of hydrogen between a bubble and melt has then the form [5]:

$$\frac{dm_{H_2}}{dt} = - \frac{0.381RTg^{1/3}\rho^{1/3} D_{H_2,eff}^{2/3}}{\eta^{1/3} p_t M_{H_2}} (L_{H_2} p_{H_2} - c_{bH_2}) \quad (18)$$

The similar interaction mechanism is assumed for CO. Here, m_{H_2} is the mass of hydrogen transported from the bubble, η and ρ are the glass viscosity and density, and $D_{H_2,eff}^{2/3}$ is the effective value of diffusion coefficient of hydrogen in the melt. The value of $D_{H_2,eff}^{2/3}$ is dependent on the redox state of glass, reflecting thus the influence of chemical reaction on the hydrogen absorption.

As the value of hydrogen bulk concentration in the melt, c_{bH_2} , is considered zero, only product $D_{H_2,eff}^{2/3} L_{H_2}$ should be known to describe the behaviour of bubbles containing hydrogen.

The experimental examination of bubble absorption presented in figures 2 - 4 can be used to this purpose. The values of the product $D_{H_2,eff}^{2/3} L_{H_2}$ calculated

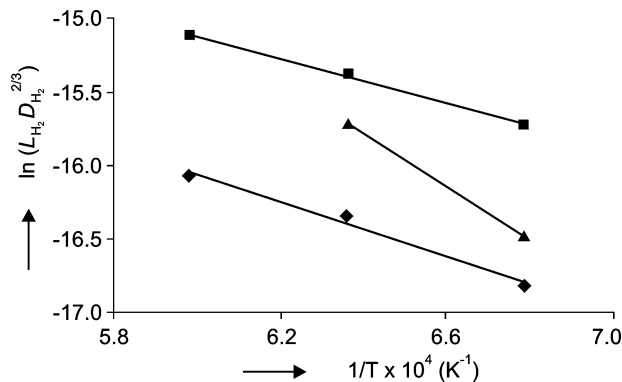


Figure 7. The temperature dependence of the logarithmic value of the product for examined glasses.

■ - glass containing 0.5 wt.% SO₃, ▲ - glass without refining agents, ◆ - amber glass

from bubble equations were used to fit the experimental data. The calculated courses of bubble diameter versus time using the optimum values of $D_{H_2,eff}^{2/3} L_{H_2}$ are as well plotted in figures 2 - 4 as dotted lines. In most cases, the theoretical and experimental courses well coincide. In figure 7, the logarithmic values of $D_{H_2,eff}^{2/3} L_{H_2}$ fit well the linear dependence versus $1/T$. For practical use of bubble modelling, the temperature dependencies have the form: $L_{H_2} D_{H_2,eff}^{2/3} = \exp(0.866-7438/T)$ for the glass containing 0.5 wt.% SO₃ and $L_{H_2} D_{H_2,eff}^{2/3} = \exp(0.946-9125/T)$ for amber glass, where L is in $\text{kg m}^{-3} \text{Pa}^{-1}$, D in $\text{m}^2 \text{s}^{-1}$ and T in Kelvins.

CONCLUSION

The results of the experimental study provided the mechanism of hydrogen transport from bubbles into a glass melt joined with the chemical reaction between oxidizing components, namely oxygen and sulphate ions, and diffusing gas. The proposed mechanism assumed the mutual equilibrium of oxidizing components in the bulk glass and the chemical reaction between reducing and oxidizing components near the bubble surface. Although the chemical reactions should evoke a supersaturation of the bubble surroundings by SO₂, no bubble nucleation was observed in experiments and no SO₂ or product of its reaction was found in bubbles. Owing to complexity of the proposed interaction mechanism and numerical solution of the appropriate equations, the simplified procedure for the description of bubble defect behaviour under real conditions was presented. The value of the product of the effective hydrogen diffusion coefficient and hydrogen solubility in the glass was determined from the presented experiments. A satisfactory agreement was achieved between experimental and computed courses of bubble absorption. The analogical behaviour is assumed for carbon monoxide containing bubbles, however, the appropriate experiments are needed to confirm their actual interaction mechanism.

Acknowledgement

This work was supplied with the subvention by The Ministry of Education, Youth and Sports of The Czech Republic, Project No. VS 96065.

References

1. Němec L., Kloužek J., Maryška M., Raková M., Šimůnková D.: *Glastechn. Ber. Glass Sci Technol.* 68 C2, 134 (1995).
2. Beerkens R.C.G.: *Glastechn. Ber.* 63K, 222 (1990).
3. Itoh E., Yoshikawa H., Kawase Y.: *Glastechn. Ber. Glass Sci. Technol.* 70, 8 (1997).
4. Yoshikawa H., Kawase Y.: *Glastechn. Ber. Glass Sci. Technol.* 70, 31 (1997).
5. Němec L., Kloužek J.: *J.Non-Crystal.Solids* 231, 152 (1998).
6. Ullrich J.: Private communication.
7. Jepsen Marwedel H., Brückner R.: *Glastechnische Fabrikationsfehler*, p.255, Springer-Verlag Berlin, Heidelberg, New York 1980.
8. Němec L., Kloužek J.: *Ceramics-Silikáty* 39, 1 (1995).

Submitted in English by the authors.

ABSORPCE VODÍKU A OXIDU UHELNATÉHO Z BUBLIN VE SKELNÉ TAVENINĚ LUBOMÍR NĚMEC, JAROSLAV KLOUŽEK

*Laboratoř anorganických materiálů, společné pracoviště
Vysoké školy chemicko-technologické a Ústavu anorganické
chemie AV ČR, Technická 5, 166 28 Praha*

Zkoumání interakcí bublin s taveninou poskytuje zajímavé údaje o mechanismech rozpouštění a reakcích plynné

fáze se skelnými taveninami a má i technologický význam při zkoumání původu bublin jako vad v průmyslově vyráběných sklech. Bubliny obsahující redukující plyny, jako je H₂ nebo CO, jsou produkovány reakcemi nečistot uhlíku a železa s kyslíkem a vodní parou při tavicím procesu skel. Experimentální sledování absorpce uměle připravených bublin obsahujících 95 obj.% H₂ a 5 obj.% N₂ v průmyslovém plochém a obalovém skle ukázalo, že řídicím dějem interakce je transport vodíku a oxidujících složek (kyslík, síranové ionty) sklovinou v okolí bubliny, ovlivněný chemickou reakcí vodíku se zmíněnými oxidujícími složkami skloviny. Navržené rovnice popisující tento děj zahrnují simultánní chemickou rovnováhu oxidujících složek ve sklovině, difúzně-konvektivní transport vodíku ze stoupající bubliny a chemickou reakci vodíku s rozpuštěným kyslíkem a síranovými ionty v tavenině.

Byl rovněž navržen zjednodušený mechanismus, který předpokládá transport vodíku bez chemické reakce a zavádí hodnotu efektivního difúzního koeficientu vodíku, závislého na oxidačně-redukčním chování skelné taveniny. S využitím zmíněných experimentálních sledování byly ze zjednodušeného modelu vypočteny součiny rozpustnosti a efektivního difúzního koeficientu vodíku. Bylo dosaženo dobré shody mezi výsledky absorpčních experimentů a zjednodušeným modelem. Získané teplotní závislosti rozpustnosti a difúzního koeficientu v oblasti 1200 - 1400 °C mají tvar: $L_{H_2}D_{H_2}^{2/3} = \exp(0.866-7438/T)$ pro sodnovápenatokrémicité sklo obsahující 0,5 hmotn.% SO₃ a $L_{H_2}D_{H_2}^{2/3} = \exp(0.946-9125/T)$ pro ambrové sklo, kde L je v kg m⁻³ Pa⁻¹, D v m² s⁻¹ a T v Kelvinech. Získané teplotní závislosti mají praktický význam pro modelování bublinových defektů ve sklářských tavicích prostorech.